Talanta 211 (2020) 120680

Contents lists available at ScienceDirect

Talanta

journal homepage: www.elsevier.com/locate/talanta

Droplet digital PCR enabled by microfluidic impact printing for absolute gene quantification

Yang Pan[a,b], Tuo Ma[a,b], Qi Meng[a,b], Yuxin Mao[a,b], Kaiqin Chu[a,b], Yongfan Men[c], Tingrui Pan[c,d], Baoqing Li[a,b,*], Jiaru Chu[a,b]

[a] Department of Precision Machinery & Precision Instrumentation, University of Science & Technology of China, Hefei, Anhui, 230027, China
[b] Key Laboratory of Precision Scientific Instrumentation of Anhui Higher Education Institutes, University of Science and Technology of China, Hefei, Anhui, 230027, China
[c] Shenzhen Institutes of Advanced Technology, Chinese Academy of Sciences, Shenzhen, Guangdong, 518055, China
[d] Department of Biomedical Engineering, University of California, Davis, 95616, USA

ARTICLE INFO

Keywords:
Digital PCR
Microfluidic impact printing
Genetic analyses

ABSTRACT

Digital PCR enabled high-sensitivity and quantitative measurements of rare biological variants. A new digital droplet-enabled PCR technology was introduced in this paper, which partitioned genetic targets into a planar nanoliter droplet array by using a microfluidic impact printer (MIP) with a disposable microfluidic chip. The accuracy of this MIP-enabled PCR technology was verified by detecting a series of concentration gradients of GAPDH gene across spanning four orders of magnitude (from 0.464 copies/μL to 464 copies/μL). Furthermore, this technology was applied to detect the expressions of p53 gene in colon cancer tissues and adjacent non-tumorous tissues, from which the copies of the nucleic acids could be absolute-quantitatively determined. The outcomes were consistent with the results of using the conventional real-time PCR, demonstrating a great potential of the MIP-enabled digital PCR in detecting gene expression in clinical samples.

1. Introduction

Detection of differential gene expression in tumors and normal tissues is one of the most widely used strategies to discover and understand cancer molecular pathways, as well as to reveal genes that prove useful for diagnosis and prognosis [1,2]. Polymerase chain reaction (PCR) has become a golden standard in the genetic detection since its emergence in 1983, due to its remarkable ability of amplifying single-molecule's concentration by replicating a large amount of target genes in a short time [3]. Among them, traditional PCR techniques, such as agarose gel electrophoresis and real-time PCR, only perform qualitative and relative detections [4,5]. While the developing digital PCR technique provides an absolute gene quantification of single molecule level, without requirement of comparison with standard reference [6,7]. Using digital PCR, the target molecules are extremely diluted and dispersed into different reaction chambers for single molecule amplification, thus the copies of the target gene can be calculated directly by counting the positive reaction chambers [8,9], which is independent of the amplification efficiency [10,11]. Due to its unique absolute quantitative ability, high accuracy and sensitivity, digital PCR has been used more and more widely in biological researches, such as detection of rare mutations [[12–14]], copy number variation [[15–17]] and next-generation sequencing [18].

In 1999, Vogelstein et al. implemented the earliest digital PCR system in multi-well plates [6]. To address the inherent defects of less reaction units, sample reagents waste and human manipulating errors, microfluidic technology was developed to conduct DNA amplification in droplets due to its unique ability of dispersing small volume droplets efficiently and automatically [[19–22]]. A number of droplet digital PCR platforms based on microfluidics have been established and commercialized for single cell analysis [23,24], early cancer diagnosis [25,26] and prenatal diagnosis [27,28]. For example, Fluidigm co. and Thermo Fisher Scientific co. used integrated microfluidic chips and specially designed silicon array chips to physically isolate liquid into independent reaction chambers, respectively; Bio-rad co. and Raindance Technologies co. used droplet microfluidic technology to produce large number of uniform water-in-oil microemulsions, where tens of thousands of parallel reactions simultaneously happen [[29–31]], and developed a droplet readout system for next digital counting. However, these commercialized digital PCR systems usually require a dedicated fabrication for complex chips, or need specialized external control of microvalves and pumps for discrete droplets generation, as well as

* Corresponding author. Department of Precision Machinery & Precision Instrumentation, University of Science & Technology of China, Hefei, Anhui, 230027, China.
E-mail address: bqli@ustc.edu.cn (B. Li).

https://doi.org/10.1016/j.talanta.2019.120680
Received 1 November 2019; Received in revised form 20 December 2019; Accepted 24 December 2019
Available online 28 December 2019
0039-9140/

expert testing equipment for signal reading. They have high stability but less flexibility to adjust the volumes and gradients of the droplets, and the high equipment cost is also a problem for individual researchers.

Besides, more explorations of developing stable, flexible and low-cost digital PCR system are being performed by scientists [14,32]. The crucial factor of the digital PCR technology is how to generate independent microreactors efficiently. Ismagilov group developed a simple, low-cost slip chip for digital PCR [33,34]. The fluidic path was broken by slipping of the precision-designed two plates that removed the overlap between wells and generated multiple reaction compartments simultaneously. Lin group [35] and He group [36] demonstrated similar flexible online digital polymerase chain reaction (dPCR) systems that generated droplets in crimped capillaries for thermal cycling and integrated a special design photodetection device for positive droplet counting. Fang group developed a novel approach which combined robotic liquid handling and specially processed hydrophilic micropillars for digital PCR [37]. It realizes a multi-volume digital PCR method by changing the liquid flow rate in the capillary and the moving speed of the chip/stage, which can achieve a wider dynamic detection range when the number of droplets is the same. Similarly, Du group reported a cross-interface emulsification technique, which can generate size-tunable droplets at the air-oil interface by changing the capillary flow rate and vibrating frequency for digital LAMP (loop mediated isothermal amplification) [38]. Table 1 summarizes the characteristics of different digital PCR methods.

In this work, we first proposed a droplet digital PCR technology based on microfluidic impact printing (MIP-ddPCR). A wide range of nanoliter droplet array was dispensed on a uniform hydrophobic quartz substrate. Then the genes dispersed in the planar droplet array were amplified using a flat thermal cycler and detected using a scanning fluorescence microscope. The concentration of the genes was therefore calculated from the fluorescence image according to the Poisson distribution theory. As a low-cost, non-contact method of generating picoliter to nanoliter droplets [40,41], the microfluidic impact printing technology uses disposable microfluidic chips to eliminate the risk of cross-contamination. Furthermore, the microfluidic impact printing technology has the ability of dispensing multiple droplets on any position to forming a multi-volume droplet PCR system, which could expand the concentration range of measurement. Specially, we verified the quantitative accuracy of the MIP-ddPCR system across four orders of magnitude by detecting a series of concentration gradients of GAPDH gene. And the digital PCR system was further applied to accurately detect the expression levels of p53 gene in colon cancer samples, revealing the potential of this method to detect single-molecule DNA.

2. Experiment

2.1. MIP-ddPCR setup

The MIP-ddPCR setup is mainly composed of three separate parts: a microfluidic printing device, a PCR amplification device and a fluorescence detection apparatus. Except for the first part, the other two parts are both general instruments in biological laboratory. Combining our previous developed microfluidic impact printing devices [40,41], we set up the droplet printing device using a piezoelectric cantilever and a microfluidic chip, along with a high-precision three-axis motorized stages (DDS220 & LTS150, Thorlabs, USA). Pulse signals were generated by a computer and a microcontroller, then amplified by a home-made high-voltage amplifier to drive the piezoelectric actuator. The droplets were printed at 10 Hz onto a quartz glass substrate, which moved with the motorized XY stages along fixed path and was kept 2 mm away from the nozzle in vertical direction, forming a droplet array or desired droplet pattern (Fig. 1a). At the same time, a CCD camera was placed under the motorized stages to observe the generated droplet morphology in real-time. In addition, a humidifier was used to keep a stable humidity (RH = 80%) in the closed environment to prevent droplet evaporation. Fig. S1a shows photograph of digital PCR technology platform based on microfluidic impact printing.

A thermal cycler (HP01, Beijing Kubo Technology Ltd., China) was used to control the DNA amplification with MATLAB software (Fig. 1b). The amplification procedure was initiated with 3 min “UNG inactivation” at 50 °C and 10 min of “hot start” at 95 °C. Since we were using AceQ®U + Probe Master Mix, we can perform the two-step PCR, which combines annealing and extension into one step. Next, the 40 thermal cycling programs were set to 35 s at 95 °C for denaturation, 75 s at 60 °C for annealing and extension. Lastly, a cross-sectional image of the droplet array was taken with a confocal microscope (CSU-X1, Nikon, Japan) (Fig. 1c) to capture the amplified gene contained in the droplet. The number of fluorescence droplets was calculated using a self-programming algorithm in MATLAB. It is noteworthy that one can use any other general fluorescence imaging device to take the place of the confocal microscope.

Table 1
Summary characteristics of different digital PCR methods.

Company/author	Dispersion method	Analysis	Minimum reaction volume	Number of reactions	Single/multi-volume	Price or cost
Fluidigm [7,39]	Microwell array	CCD camera – real time PCR end point melting curve analysis	0.85 nL	36,960	Single	$100,000-$150,000 $800 per chip
Thermo Fisher Scientific [7,39]	Microwell array	CCD camera – real time PCR end point melting curve analysis	33 nL	3072	Single	$90,000-$190,000 $150 per plate
Bio-Rad [7,39]	Water-in-oil microemulsion	Automated droplet flow cytometer	1 nL	20,000	Single	$89,000 $3 per sample
RainDance [7,39]	Water-in-oil microemulsion	End point analysis	5 pL	10,000,000	Single	$100,000 $10–$30 per sample
He group [36]	Water-in-oil microemulsion	Capillary-based flow cytometer	About 14 pL	/	Single	/
Lin group [35]	Inkjet-based droplet-generating	Laser-induced fluorescence detector	About 65 pL	/	Multi-	/
Ismagilov group [34]	Slip Chip	End point analysis	0.2 nL	880	Multi-	/
Fang group [37]	Sequential Operation Droplet Array (SODA)	CCD camera – end point analysis	1.2 nL	994	Multi-	/
Du group [38]	Cross-interface emulsification	CMOS camera - end point analysis	0.2 nL	/	Multi-	/
Our work	Microfluidic Impact Printing	End point analysis	2.5 nL	1000 per channel	Multi-	< $5000

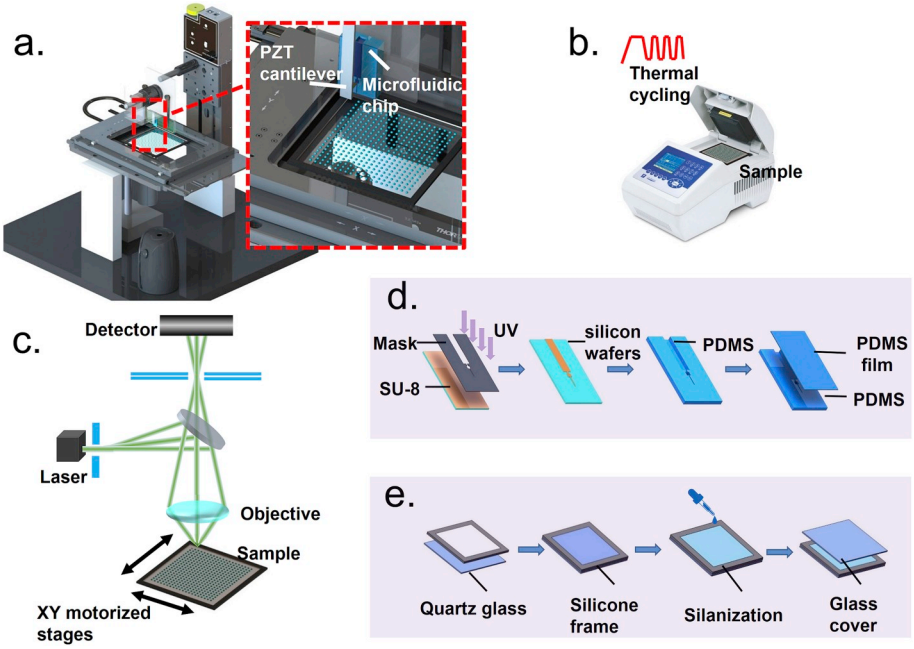

Fig. 1. Schematic diagrams of a microfluidic printing droplet digital PCR setup (MIP-ddPCR setup), which is composed of (a) the microfluidic printer, (b) a flat thermal cycler and (c) a fluorescence microscope. Schematic diagrams of (d) the manufacturing process of a disposable microfluidic printing chip and (e) the manufacturing process of a hydrophobic quartz substrate.

2.2. Chip fabrication and substrate packaging

The microfluidic chip is designed using the AutoCAD software and fabricated by soft lithography techniques. Specifically, SU-8 2050 photoresist was spin-coated onto a silicon wafer, patterned by UV exposure through a photolithography mask. Then a 10:1 (w/w) mixture of the polydimethylsiloxane (PDMS) prepolymer and curing agent (Dow Corning SYLGARD184, USA) was degassed under vacuum for 15min, and poured over to a height of about 3 mm, forming a structured microfluidic substrate. After curing for 2 h at 65 °C, PDMS was gently peeled off from the master, the structured side of the PDMS was bonded to a 250 μm-thick of planar PDMS film through oxygen plasma treatment (Mingheng PDC-MG, China) at 75 W and 60Pa for 50s. Finally, a scalpel was used to cut the print chip nozzle under a microscope (Fig. 1d). Fig. S1b shows photograph of a disposable microfluidic chip.

The double-layer hydrophobic glass substrate is composed of a 1 mm thick silicone pad and a quartz glass plate (5 cm × 5 cm × 1 mm). The silicone pad was cut into a frame (internal size 4 cm × 4 cm) to prevent oil from spilling, and bonded to glass through oxygen plasma treatment (Mingheng PDC-MG, China) at 75 W and 60Pa for 50s. The quartz glass was silanized in ethanol containing trifluorosilane ((1H, 1H, 2H, 2H-perfluorooctyl), 0.0625% v/v, Sigma, USA) for 5 min and the contact angle of the glass was optimized to 81.2° (Fig. S2). This angle not only makes the droplets have a good adhesion with the silanized glass, but also prevents the droplets from contamination between each other. After completion of droplet printing, 1 mL mineral oil (M5940, Sigma, USA) was filled into the frame-bonded quartz glass to fully overlay the droplets. Owning to the lower density of the mineral oil (0.84 g/mL), the droplets can be fully covered by the oil to prevent water evaporation. Finally a glass was placed on the frame for further protection during thermal cycling (Fig. 1e). Fig. S1c shows a photograph of a hydrophobically treated quartz substrate.

2.3. The optical detection apparatus

In order to explore suitable amplification conditions, we have built a real-time fluorescent PCR detection setup, which consists of a series of optical devices and an additional imaging system. The optical setup consisted of a CCD camera (DP72, Olympus, Japan), a 4 × objective lens (Olympus, Japan), a filter (Semrock, Japan) set of 460/20 nm for fluorescence excitation and 532/30 nm for emission collection of the FAM dye. All fluorescent images were processed by ImageJ (National Institutes of Health, USA) to obtain the fluorescence intensity value of each droplet. These values were then normalized, and the real-time PCR values were calculated. To evaluate the precision of the droplet size, a high-speed stroboscopic microscope (Photron FASTCAM SA5, Japan) with 8 × magnification was used to capture the images of the printed droplets. Then, the images were batch analyzed in the MATLAB (2017a) to measure the diameter and calculated the coefficient of variation (CV) of the droplets. Fig. S1d shows photograph of real-time fluorescent PCR detection device.

2.4. Biological experiments

GAPDH is a house-keeping gene, which is expressed at a high level in almost all tissues, and the protein expression in the same cells or tissues is constant. Therefore, it is widely used as a reference gene and is also used to verify the feasibility of digital PCR [37]. The MIP-ddPCR system was tested using a serial dilution of the stock DNA spanning four of magnitude from $1{:}10^4$ to $1{:}10^7$. Each 20 μL PCR master mixture consisted of 10 μL of AceQ®U + Probe Master Mix (2 ×) (Vazyme, China), which contains Heat-labile UDG anti-pollution system. UDG is uracil DNA glycosylase, which can quickly degrade UTP-containing DNA templates at room temperature, and effectively prevent PCR product from contamination. 1 μL of GAPDH primer (FAM dye) mix (20 ×) (Hs02758991_g1, ThermoFisher Scientific Inc., USA), 2 μL of standard GAPDH plasmid template solution (Sangon Biotech, China, concentration is 4.64 × 10^7copies/μL), 6 μL of RNase-free water, and 1 μL of 20 mg/mL bovine serum albumin (BSA) solution.

For the detection of the p53 gene, RNA was extracted from colon cancer tissues (School of Life Sciences, USTC) with chloroform. Then cDNA was got from the reverse transcription kit (Takara, Japan). Each 20 μL PCR master mixture consisted of 10 μL of AceQ®U + Probe Master Mix (2 ×), 1 μL of p53 primer (FAM dye) mix (20 ×) (Hs01034249_m1, ThermoFisher Scientific Inc., USA), 2 μL of cDNA (diluted in DEPC-water (Sangon Biotech, China)), 6 μL of RNase-free water, and 1 μL of 20 mg/mL bovine serum albumin (BSA) solution. Reverse transcription program settings were 37 °C for 15 min, 85 °C for 15s. Detection of p53 gene was using commercial qPCR instrument (Thermo Fisher, USA) for comparison with MIP-ddPCR technology.

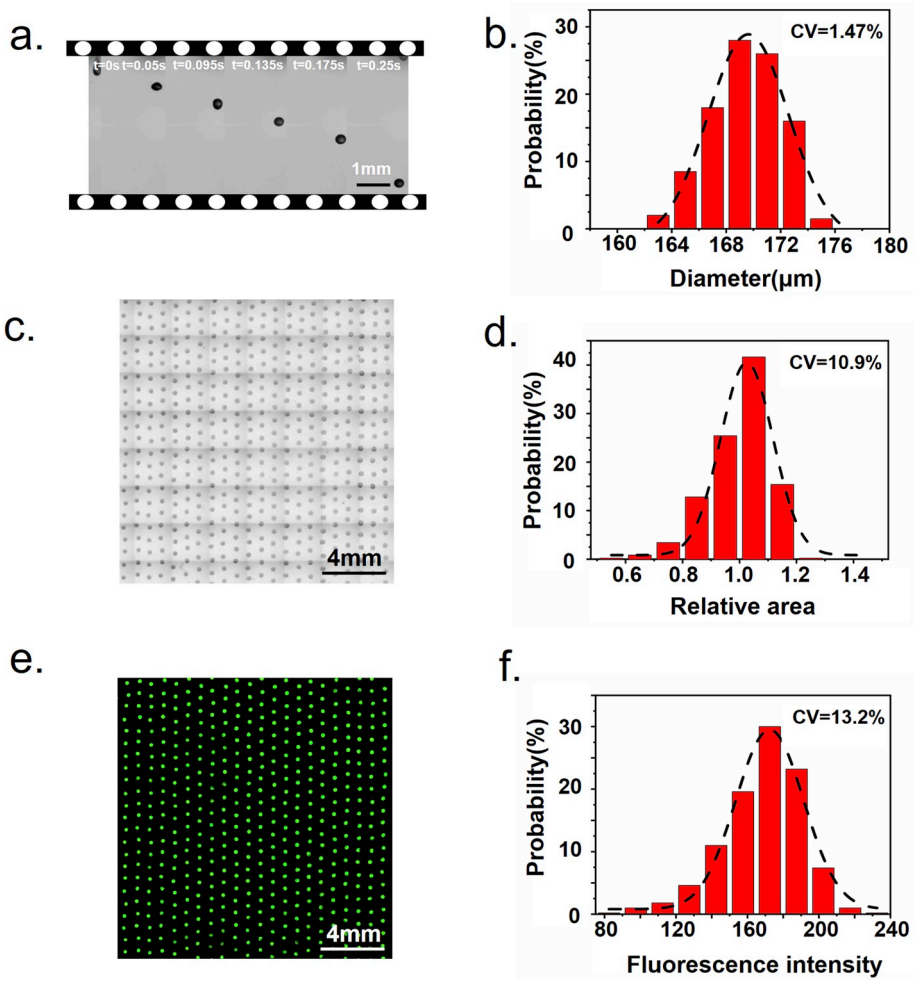

Fig. 2. (a) Stroboscopic images showing the DI water droplet printing process (scale bar: 1 mm) and (b) probability distribution histograms of the droplet diameters. (c) Optical image of the droplet array on a quartz chip (scale bar: 4 mm) and (d) probability distribution histograms of the droplet areas. (e) Fluorescence image of 0.1 mg/mL sodium fluorescein droplet array on a quartz chip (scale bar: 4 mm) and (f) probability distribution histograms of droplet intensities.

3. Results and discussion

3.1. Evaluation of the performance of the generated droplets

For digital PCR, the volumetric uniformity of each compartmentalization is of significant importance for the concentration of DNA template molecules is directly calculated from their distribution in containers with assumed equal volumes. Here we used a high-speed photography to verify the volumetric uniformity of printed droplets, and analyzed the coefficient of variation by image processing. 260 DI water droplets generated from the microfluidic printer were captured using a stroboscope. Fig. 2a shows the stroboscopic images during droplet printing process. With an impact action of the piezoelectric actuator, one droplet is ejected from the nozzle. The size distribution of the droplet diameters is displayed by a histogram in Fig. 2b, which shows an average diameter of 170 μm with coefficient of variation (CV) of 1.47%, demonstrating a good monodispersity of droplets generated by microfluidic printing. And the calculated average volume is about 2.5 nL with CV of 4.4%.

To further examine the uniformity of the droplets on the substrate, we configured a low concentration (dilute to 0.1 mg/mL with deionized water) of sodium fluorescein ($C_{20}H_{10}Na_2O_5$) solution as a calibrator to produce droplet array on a hydrophobically modified glass substrate. Fig. 2c shows the optical image of droplet array. The CV (=10.9%) of the droplet areas shown in Fig. 2d was obviously enlarged. This is mainly due to the morphological changes during the droplets falling onto substrate and oil covering. The shapes of the droplets on the quartz substrate weren't as uniform as they were in the air. In addition, we measured the fluorescence intensities of droplets on substrate. As shown in Fig. 2e and f and , the calculated CV was 13.2%, a little larger than the optical value. It is indicated that in the MIP-ddPCR, the measured fluorescence intensity difference between the positive and negative containers (droplets) must be large enough to be distinguished, since the DNA concentration is calculated by counting number of the positive droplets.

3.2. Real-time PCR analysis

To investigate the amplification parameters of the droplet PCR using a flat thermal cycling platform, a real-time fluorescence detection setup was established as shown in Fig. 3a. A 3 by 3 droplet array was generated by MIP and oil covered on a silanized quartz substrate. Then the thermal cycle program was set to 35 s at 95 °C, 75 s at 60 °C for 40 cycles. Observed from the experiments, the positive droplets are obviously amplified (Fig. 3b), similar in the trend to the traditional qPCR method. The results showed that the droplets were amplified and reached the plateau after 37 cycles, while the positive and negative droplets showed significant contrast of more than three times, which laid a good experimental foundation for the subsequent digital PCR experiments.

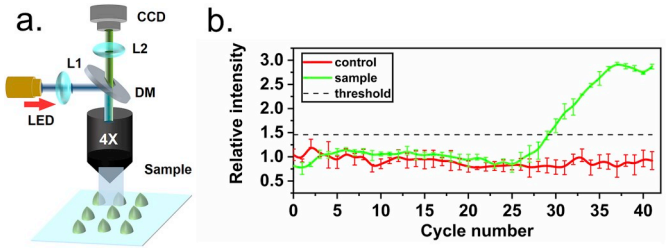

Fig. 3. Real-time PCR detection of droplets. (a) Schematic diagram of real-time fluorescent PCR detection device. (b) Real-time amplification of positive fluorescent droplets and negative fluorescent droplets. The green line is a positive curve and the red line is a negative curve, indicating that the fluorescence intensity of the positive droplet amplification is significantly enhanced compared to the negative droplet. Threshold is 10 × the standard deviation of background. (For interpretation of the references to colour in this figure legend, the reader is referred to the Web version of this article.)

3.3. Performance of the MIP-ddPCR

A series of diluted GAPDH plasmid DNA solutions spanning three orders of magnitude from 1:10^4 to 1:10^6 were generated and implemented using the MIP-ddPCR to verify its absolute quantitative performance (Fig. 4). The PCR mixture was prepared in advance and all ingredients were premixed prior to dripping onto the substrate. During amplification, the fluorescence intensities of the negative droplets containing no DNA molecules had little change. Only the droplets containing target DNA molecules would accumulate fluorescence as a result of TaqMan probe cleavage, the average intensity of which was three times that of the negative droplets, ensuring an obvious distinguish between positive and negative droplets (Fig. S3a). Fig. 4a–e shows fluorescent images of a negative control and four different concentrations of 25 by 40 droplet array. Number of positive droplets increases with the DNA concentration. Details of the intensity distributions are shown in Fig. S3.

In the experiments, there may be two or more DNA molecules in one droplet. Therefore, it is necessary to calculate the number of DNA accurately by mathematical correction of the Poisson distribution [42]. According to the Poisson distribution formula: $\lambda = -\ln(1-p)$, we can get the relationship between the expected fraction of the positive droplets p and the average number of DNA template copies per droplet λ, so as to calculate the DNA concentration. As shown in Fig. 4f, the results show that the measured concentration in the experiment has a good correlation with the actual concentration (R^2 = 0.997), which verifies the feasibility of MIP-ddPCR system in quantitation of gene targets.

In conventional pump-based droplet formation process, a large amount of expensive biological reagent was wasted for it needs a period to stabilize the flow process before uniform droplet generation. Moreover, the reagent always remains in the connecting tube and the chip channel due to the physical separation between the droplet generating chip and the injectors [43]. Additionally, in biological applications, sample waste is unacceptable, such as single-cell whole-genome sequencing. Remarkably, the least volume of the reagent used for our droplet array generation is less than 2.7 μL with a tiny dead volume of 0.2 μL here, which means utilization ratio of the reagent is more than 92.6%.

The measurable concentration range of digital PCR in uniform volume is usually limited by the number of droplets. Therefore, a lot of digital PCR methods expand their detection range by increasing the number of reaction units. On the other side, multi-volume digital PCR can significantly reduce the total number of reactors and achieve a wider dynamic range [44]. Thanks for the in-situ printing ability of MIP-ddPCR system, we set larger reaction system volume by printing multiple droplets on each position. Here, a 20 by 20 drop array with each drop volume of 70 nL is printed within 4 min for detecting lower DNA concentrations (Fig. 5a). The DNA expression achieved in positive droplets was clearly distinguished by nearly three times the fluorescence intensity of the negative droplets (Fig. S4a). Fig. 5b shows that the measured concentration is in good agreement with the actual concentration (R^2 = 0.995). This indicates that the increased droplet volume can further expand the detection range of MIP-ddPCR technology and detect a lower order of DNA concentration. In other words, the multi-volume digital PCR technology can be used to detect samples with larger differences in concentration by changing the volume of the droplets. And it can reduce the dilution processes of detection samples with unknown concentration.

3.4. P53 genes detected by MIP-ddPCR system

Cancer has become a major public health problem worldwide, with high morbidity and high mortality rates [45]. Recent statistics show

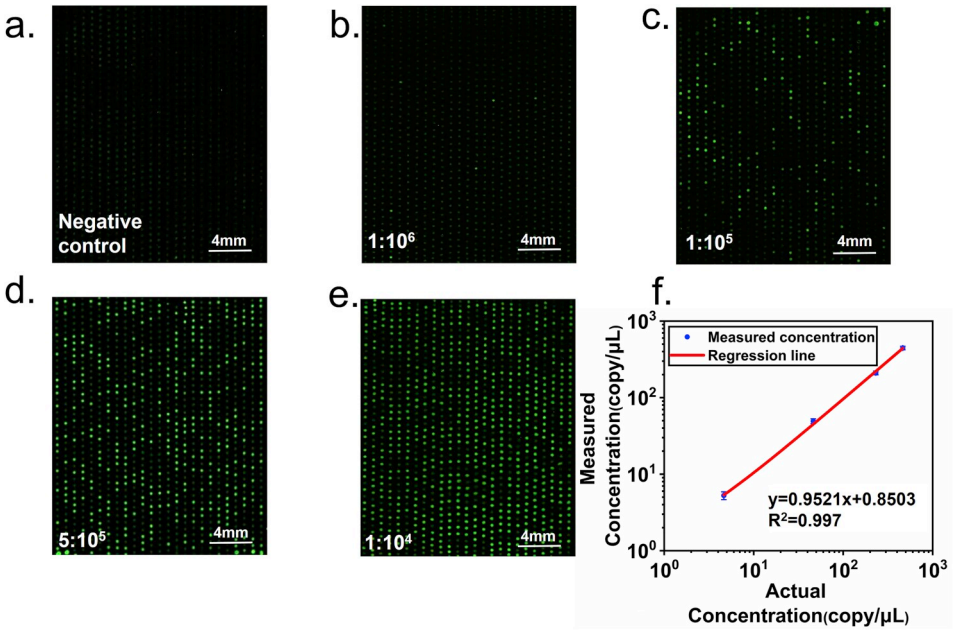

Fig. 4. MIP-ddPCR results for a series of dilution concentrations of GAPDH. For each concentration, the experiment was repeated three times. (a) A control group, which is without DNA template, shows no positive result. (b)–(e) A series of dilutions of GAPDH plasmid DNA from 1:10^4 to 1:10^6 as experimental group. As the concentration increases, more positive droplets are observed (scale bar: 4 mm). (f) The concentration of the DNA template calculated from the number of positive droplets, where the observed concentration matches well with the actual concentration according to the Poisson distribution (R^2 = 0.997).

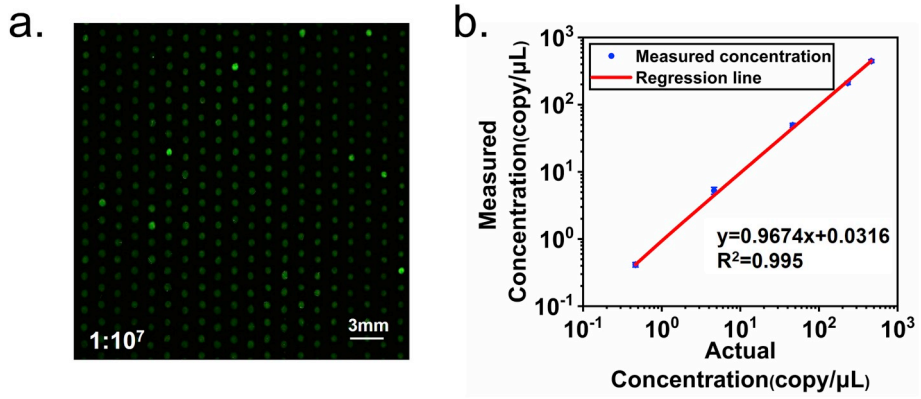

Fig. 5. (a) 20 by 20 drop array with each drop volume of 70 nL (concentration diluted $1:10^7$) (scale bar: 3 mm). (b) According to the Poisson distribution, the observed concentration agrees well with the actual concentration ($R^2 = 0.995$) and expands the detection range by an order of magnitude.

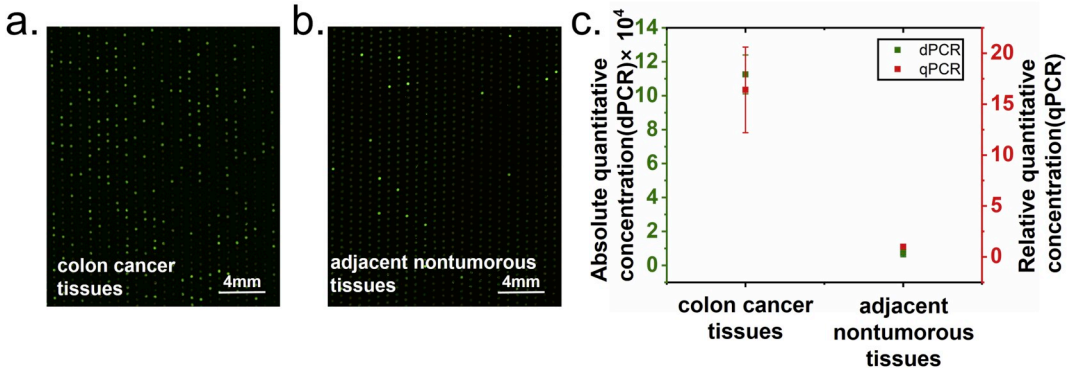

Fig. 6. Fluorescence images of colon cancer tissues (a) and adjacent nontumorous tissues (b), which were detected by MIP-ddPCR technology (scale bar: 4 mm). (c) Absolute quantitative concentration analysis of colon cancer tissues and adjacent nontumor tissues by MIP-ddPCR technology and relative quantitative concentration analysis of colon cancer tissues and adjacent non-tumor tissues by commercial qPCR technology.

that the p53 genes is overexpressed in colon cancer tissues, which has been demonstrated as an independent predictor of tumor recurrence in colon cancer patients [[46–49]]. Here, we use the MIP-ddPCR technology to detect the expression of p53 gene in colon tumor tissues and adjacent nontumorous tissues [50,51]. We extracted RNA from tissue samples, and obtained their cDNA by reverse transcription, while the housekeeping GAPDH gene was used to normalize the amount of different input cDNA from different tissues. The PCR mixture was configured with cDNA as a template, and the p53 copies were detected by the MIP-ddPCR setup (Fig. 6a and b) and commercial qPCR instrument. As shown in Fig. 6c, p53 was highly expressed in tumor tissues, and the copies of p53 gene in tumor tissues was 1.1×10^5 copies/mL, which was one order of magnitude higher than that in nontumorous tissues (7.2×10^3 copies/mL). The presence of larger concentration of p53 gene in the colon tumor indicates a significant association between p53 expression levels and colon cancer. And this result is consistent with the that of qPCR experiments. However, different from the relative quantification by qPCR, the absolute quantitation of the copies of cDNA can be directly achieved by the MIP-ddPCR, which plays an important role in the detection of differential gene expression in tumors and normal tissues. Different tumor grades are associated with distinct gene expression profiles. Accurate and quantitative detection of the differential gene expression helps to gain insight into the extent of expression differences underlying malignancy and provides a quantitative standard for cancer-associated marker genes that does not require a reference. Overall, our MIP-ddPCR technology has great potential as a tool for the analysis of biological diagnosis related gene expression of cancer patients.

4. Conclusions

In summary, we develop an absolute quantitative digital PCR technology by dispersing, amplifying and detecting target genes in planar droplet array. This technology provides a simple and lab-affordable method to perform high-sensitivity absolute genetic analysis for researchers in the biological laboratory, since the droplet digital PCR setup uses only a low-cost microfluidic printer, combined with other general laboratory instruments, i.e. an in-situ PCR device and a fluorescence microscope are enough. As a non-contact and cross-contamination free method of generating picoliter to nanoliter droplets, the microfluidic impact printing technology has no requirement of external pumps and valves which are usually adopted by other digital PCR methods. And it has high utilization ratio of the expensive biological reagents (> 92.6%), which is especially suitable for the detection of rare bio-targets. The droplets are generated from a disposable microfluidic chip, saving the tiresome washing process for operators. Moreover, using printing method to generate addressable microdroplets on planar substrate provides convenience of marking and extracting target objects in subsequent experiments, as well as controlling the volume of each droplet container.

DNA templates across four orders of magnitude have been accurately detected by using the MIP-ddPCR, and this concentration range could be further expanded through dispensing multi-volume droplet containers using the microfluidic printing. In addition, we found that this method can distinguish between cancer and normal tissues by detecting cancer markers, which confirms its clinical application potential.

Limited by the working area of the thermal cycler, the droplet array currently can only contain one thousand droplets on the slide. Furthermore, genetic analyses on a larger array of droplets can be realized by using a flatbed thermal cycler with a larger footprint. In addition, this printing system can be loaded with multiple channels, which provides a high-throughput droplet generation ability. Such a fully automated and highly adaptive PCR technology has great potential to be applicable to a wide range of biomedical applications, such as early diagnosis of cancer, non-invasive prenatal diagnosis, single cell analysis, high-throughput drug screening and etc.

Acknowledgments

This research work has been supported in part by National Natural Science Foundation of China (No. 51675505), Joint Research Fund for Overseas Chinese Scholars and Scholars in Hong Kong and Macao (No. 51929501), and Program for Guangdong Introducing Innovative and Entrepreneurial Teams (2016ZT06D631), and Shenzhen Fundamental Research Program (JCYJ20170413164102261). The authors would like to acknowledge the USTC Experimental Center of Engineering and Material Sciences and the USTC center for Micro-and Nanoscale Research and Fabrication for technical support in microfabrication. Also Mr. Xianchong Yin's assistance in the image processing program is appreciated.

Appendix A. Supplementary data

Supplementary data to this article can be found online at https://doi.org/10.1016/j.talanta.2019.120680.

References

[1] L. Zhang, W. Zhou, V.E. Velculescu, S.E. Kern, R.H. Hruban, S.R. Hamilton, B. Vogelstein, K.W. Kinzler, Gene expression profiles in normal and cancer cells, Science 276 (5316) (1997) 1268–1272.
[2] P. Liang, A.B. Pardee, Analysing differential gene expression in cancer, Nat. Rev. Cancer 3 (11) (2003) 869–876.
[3] L.H. Lauerman, Advances in PCR technology, Anim. Health Res. Rev. 5 (2) (2004) 247–248.
[4] S.A. Bustin, T. Nolan, Pitfalls of quantitative real-time reverse-transcription polymerase chain reaction, J. Biomol. Tech. 15 (3) (2004) 155–166.
[5] S.A. Bustin, R. Mueller, Real-time reverse transcription PCR (qRT-PCR) and its potential use in clinical diagnosis, Clin. Sci. 109 (4) (2005) 365–379.
[6] B. Vogelstein, K.W. Kinzler, Digital PCR, Proc. Natl. Acad. Sci. U. S. A. 96 (16) (1999) 9236–9241.
[7] M. Baker, Digital PCR hits its stride, Nat. Methods 9 (6) (2012) 541–544.
[8] P.J. Sykes, S.H. Neoh, M.J. Brisco, E. Hughes, J. Condon, A.A. Morley, Quantitation of targets for PCR by use of limiting dilution, Biotechniques 13 (3) (1992) 444–449.
[9] P.H. Dear, P.R. Cook, Happy mapping - linkage mapping using a physical analog of meiosis, Nucleic Acids Res. 21 (1) (1993) 13–20.
[10] A.S. Whale, J.F. Huggett, S. Cowen, V. Speirs, J. Shaw, S. Ellison, C.A. Foy, D.J. Scott, Comparison of microfluidic digital PCR and conventional quantitative PCR for measuring copy number variation, Nucleic Acids Res. 40 (11) (2012) e82.
[11] S.C. Taylor, G. Laperriere, H. Germain, Droplet Digital PCR versus qPCR for gene expression analysis with low abundant targets: from variable nonsense to publication quality data, Sci. Rep. 7 (1) (2017) 2409.
[12] J. Wang, R. Ramakrishnan, Z. Tang, W. Fan, A. Kluge, A. Dowlati, R.C. Jones, P.C. Ma, Quantifying EGFR alterations in the lung cancer genome with nanofluidic digital PCR arrays, Clin. Chem. 56 (4) (2010) 623–632.
[13] L. Dong, S. Wang, B. Fu, J. Wang, Evaluation of droplet digital PCR and next generation sequencing for characterizing DNA reference material for KRAS mutation detection, Sci. Rep. 8 (1) (2018) 9650.
[14] Z.H. Wu, Y.N. Bai, Z.L. Cheng, F.M. Liu, P. Wang, D.W. Yang, G. Li, Q.H. Jin, H.J. Mao, J.L. Zhao, Absolute quantification of DNA methylation using microfluidic chip-based digital PCR, Biosens. Bioelectron. 96 (2017) 339–344.
[15] F.Z. Marques, P.R. Prestes, L.B. Pinheiro, K. Scurrah, K.R. Emslie, M. Tomaszewski, S.B. Harrap, F.J. Charchar, Measurement of absolute copy number variation reveals association with essential hypertension, BMC Med. Genomics 7 (2014) 44.
[16] S. Robinson, M. Follo, D. Haenel, M. Mauler, D. Stallmann, L. Andreas, T. Helbing, D. Duerschmied, K. Peter, C. Bode, I. Ahrens, M. Hortmann, Chip-based digital PCR as a novel detection method for quantifying microRNAs in acute myocardial infarction patients, Acta Pharmacol. Sin. 39 (7) (2018) 1217–1227.
[17] Y. Bai, Y. Qu, Z. Wu, Y. Ren, Z. Cheng, Y. Lu, J. Hu, J. Lou, J. Zhao, C. Chen, H. Mao, Absolute quantification and analysis of extracellular vesicle lncRNAs from the peripheral blood of patients with lung cancer based on multi-colour fluorescence chip-based digital PCR, Biosens. Bioelectron. 142 (2019) 111523.
[18] R.A. White, P.C. Blainey, H.C. Fan, S.R. Quake, Digital PCR provides sensitive and absolute calibration for high throughput sequencing, BMC Genomics 10 (2009) 116.
[19] F. Shen, W.B. Du, E.K. Davydova, M.A. Karymov, J. Pandey, R.F. Ismagilov, Nanoliter multiplex PCR arrays on a SlipChip, Anal. Chem. 82 (11) (2010) 4606–4612.
[20] K.A. Heyries, C. Tropini, M. VanInsberghe, C. Doolin, O.I. Petriv, A. Singhal, K. Leung, C.B. Hughesman, C.L. Hansen, Megapixel digital PCR, Nat. Methods 8 (8) (2011) 649-U64.
[21] E.A. Ottesen, J.W. Hong, S.R. Quake, J.R. Leadbetter, Microfluidic digital PCR enables multigene analysis of individual environmental bacteria, Science 314 (5804) (2006) 1464–1467.
[22] D. Pekin, Y. Skhiri, J.C. Baret, D. Le Corre, L. Mazutis, C. Ben Salem, F. Millot, A. El Harrak, J.B. Hutchison, J.W. Larson, D.R. Link, P. Laurent-Puig, A.D. Griffiths, V. Taly, Quantitative and sensitive detection of rare mutations using droplet-based microfluidics, Lab Chip 11 (13) (2011) 2156–2166.
[23] E.A. Ottesen, J.W. Hong, S.R. Quake, J.R. Leadbetter, Microfluidic digital PCR enables multigene analysis of individual environmental bacteria, Science 314 (5804) (2006) 1464–1467.
[24] S.N. Dahotre, Y.M. Chang, A.M. Romanov, G.A. Kwong, DNA-barcoded pMHC tetramers for detection of single antigen-specific T cells by digital PCR, Anal. Chem. 91 (4) (2019) 2695–2700.
[25] W. Zhou, S.N. Goodman, G. Galizia, E. Lieto, F. Ferraraccio, C. Pignatelli, C.A. Purdie, J. Piris, R. Morris, D.J. Harrison, P.B. Paty, A. Culliford, K.E. Romans, E.A. Montgomery, M.A. Choti, K.W. Kinzler, B. Vogelstein, Counting alleles to predict recurrence of early-stage colorectal cancers, Lancet 359 (9302) (2002) 219–225.
[26] A. Vannitamby, S. Hendry, L. Irving, D. Steinfort, S. Bozinovski, Novel multiplex droplet digital PCR assay for scoring PD-L1 in non-small cell lung cancer biopsy specimens, Lung Cancer 134 (2019) 233–237.
[27] B.G. Zimmermann, S. Grill, W. Holzgreve, X.Y. Zhong, L.G. Jackson, S. Hahn, Digital PCR: a powerful new tool for noninvasive prenatal diagnosis? Prenat. Diagn. 28 (12) (2008) 1087–1093.
[28] C.R. Tan, X.H. Chen, F. Wang, D. Wang, Z.F. Cao, X.R. Zhu, C. Lu, W.J. Yang, N. Gao, H.F. Gao, Y. Guo, L.X. Zhu, A multiplex droplet digital PCR assay for noninvasive prenatal testing of fetal aneuploidies, Analyst 144 (7) (2019) 2239–2247.
[29] L. Mazutis, A.F. Araghi, O.J. Miller, J.C. Baret, L. Frenz, A. Janoshazi, V. Taly, B.J. Miller, J.B. Hutchison, D. Link, A.D. Griffiths, M. Ryckelynck, Droplet-based microfluidic systems for high-throughput single DNA molecule isothermal amplification and analysis, Anal. Chem. 81 (12) (2009) 4813–4821.
[30] N.R. Beer, B.J. Hindson, E.K. Wheeler, S.B. Hall, K.A. Rose, I.M. Kennedy, B.W. Colston, On-chip, real-time, single-copy polymerase chain reaction in picoliter droplets, Anal. Chem. 79 (22) (2007) 8471–8475.
[31] F. Schuler, F. Schwemmer, M. Trotter, S. Wadle, R. Zengerle, F. von Stetten, N. Paust, Centrifugal step emulsification applied for absolute quantification of nucleic acids by digital droplet RPA, Lab Chip 15 (13) (2015) 2759–2766.
[32] P. Wang, F. Jing, G. Li, Z. Wu, Z. Cheng, J. Zhang, H. Zhang, C. Jia, Q. Jin, H. Mao, J. Zhao, Absolute quantification of lung cancer related microRNA by droplet digital PCR, Biosens. Bioelectron. 74 (2015) 836–842.
[33] F. Shen, W.B. Du, J.E. Kreutz, A. Fok, R.F. Ismagilov, Digital PCR on a SlipChip, Lab Chip 10 (20) (2010) 2666–2672.
[34] F. Shen, B. Sun, J.E. Kreutz, E.K. Davydova, W.B. Du, P.L. Reddy, L.J. Joseph, R.F. Ismagilov, Multiplexed quantification of nucleic acids with large dynamic range using multivolume digital RT-PCR on a rotational SlipChip tested with HIV and hepatitis C viral load, J. Am. Chem. Soc. 133 (44) (2011) 17705–17712.
[35] W.F. Zhang, N. Li, D. Koga, Y. Zhang, H.L. Zeng, H. Nakajima, J.M. Lin, K. Uchiyama, Inkjet printing based droplet generation for integrated online digital polymerase chain reaction, Anal. Chem. 90 (8) (2018) 5329–5334.
[36] J. Chen, Z. Luo, L. Li, J. He, L. Li, J. Zhu, P. Wu, L. He, Capillary-based integrated digital PCR in picoliter droplets, Lab Chip 18 (3) (2018) 412–421.
[37] W.W. Liu, Y. Zhu, Y.M. Feng, J. Fang, Q. Fang, Droplet-based multivolume digital polymerase chain reaction by a surface-assisted multifactor fluid segmentation approach, Anal. Chem. 89 (1) (2017) 822–829.
[38] P. Xu, X. Zheng, Y. Tao, W.B. Du, Cross-interface emulsification for generating size-tunable droplets, Anal. Chem. 88 (6) (2016) 3171–3177.
[39] E. Day, P.H. Dear, F. McCaughan, Digital PCR strategies in the development and analysis of molecular biomarkers for personalized medicine, Methods 59 (1) (2013) 101–107.
[40] J. Fan, Y. Men, K. Hao Tseng, Y. Ding, Y. Ding, F. Villarreal, C. Tan, B. Li, T. Pan, Dotette: programmable, high-precision, plug-and-play droplet pipetting, Biomicrofluidics 12 (3) (2018) 034107.
[41] Y.X. Mao, Y. Pan, X. Li, B.Q. Li, J.R. Chu, T.R. Pan, High-precision digital droplet pipetting enabled by a plug-and-play microfluidic pipetting chip, Lab Chip 18 (18) (2018) 2720–2729.
[42] A.S. Basu, Digital assays Part I: partitioning statistics and digital PCR, Slas Technol 22 (4) (2017) 369–386.
[43] X.R. Li, D.F. Zhang, W.D. Ruan, W.Z. Liu, K. Yin, T. Tian, Y.P. Bi, Q.Y. Ruan, Y. Zhao, Z. Zhu, C.Y. Yanet, Centrifugal-driven droplet generation method with minimal waste for single-cell whole genome amplification, Anal. Chem. 91 (21) (2019) 13611–13619.
[44] J.E. Kreutz, T. Munson, T. Huynh, F. Shen, W.B. Du, R.F. Ismagilov, Theoretical design and analysis of multivolume digital assays with wide dynamic range validated experimentally with microfluidic digital PCR, Anal. Chem. 83 (21) (2011) 8158–8168.
[45] R.L. Siegel, K.D. Miller, A. Jemal, Cancer statistics, Ca - Cancer J. Clin. 68 (1) (2018) 7–30 2018.
[46] M.L. Gope, M. Chun, R. Gope, Comparative study of the expression of Rb and p53

genes in human colorectal cancers, colon carcinoma cell lines and synchronized human fibroblasts, Mol. Cell. Biochem. 107 (1) (1991) 55–63.
[47] M. Szybka, M. Zakrzewska, P. Rieske, G. Pasz-Walczak, D. Kulczycka-Wojdala, I. Zawlik, R. Stawski, D. Jesionek-Kupnicka, P.P. Liberski, R. Kordek, cDNA sequencing improves the detection of P53 missense mutations in colorectal cancer, BMC Canc. 9 (2009) 278.
[48] J.W. Huh, H.R. Kim, Y.J. Kim, Prognostic role of p53 messenger ribonucleic acid expression in patients after curative resection for stage I to III colorectal cancer: association with colon cancer stem cell markers, J. Am. Coll. Surg. 216 (6) (2013) 1063–1069.
[49] D.Z. Cao, X.L. Ou, T. Yu, The association of p53 expression levels with clinicopathological features and prognosis of patients with colon cancer following surgery, Oncology letters 13 (5) (2017) 3538–3546.
[50] X.L. Li, J.B. Zhou, Z.R. Chen, W.J. Chng, p53 mutations in colorectal cancer- molecular pathogenesis and pharmacological reactivation, World J. Gastroenterol. 21 (1) (2015) 84–93.
[51] T. Takayama, K. Miyanishi, T. Hayashi, Y. Sato, Y. Nirrsu, Colorectal cancer: genetics of development and metastasis, J. Gastroenterol. 41 (3) (2006) 185–192.